Science and Technology Indonesia
e-ISSN:2580-4391 p-ISSN:2580-4405
Vol. 6, No. 2, April 2021

Review Paper

Review of The Effectiveness of Plant Media Extracts in Barium Hexaferrite Magnets ($BaFe_{12}O_{19}$)

Jaya Edianta[1], Nanang Fauzi[1], Marzuki Naibaho[1], Fitri Suryani Arsyad[1]*, Idha Royani[1]

[1]*Department of Physics, Faculty of Mathematics and Natural Science, University of Sriwijaya, South Sumatera, Indonesia*
***Corresponding author**: fitri_suryani@unsri.ac.id

Abstract
Betel leaf is a typical Indonesian herbal plant that propagates on other tree trunks. So far, betel leaf has only been used in biomedicine and traditional medicine, whereas the chemical compounds of betel leaf can be used to absorb electromagnetic waves. In this mini-review, we review several research results to discuss the potential effectiveness of betel leaf in barium hexaferrite as an absorber of electromagnetic radiation. We compiled this mini-review based on the literature review method that is discussed extensively and in-depth regarding the chemical composition of betel leaf, modification of the development of barium hexaferrite material with betel leaf media extract, characteristics of $BaFe_{12}O_{19}$ as absorption of electromagnetic waves, and the effectiveness of media extracts in $BaFe_{12}O_{19}$ as absorption of electromagnetic waves. Based on the results of the literature review, the modification of $BaFe_{12}O_{19}$ material synthesis can include microemulsion, solid-state, coprecipitation, sol-gel, and hydrothermal synthesis. So far, hydrothermal synthesis is a synthesis method of mixing betel leaf extract media and ferrite-based magnets that have been studied before. Betel leaf in ferrite-based magnetic materials has been studied not to damage the surface morphology and characteristics of the magnetic material. The results of the assessment also show the effectiveness of adding other elements or compounds such as Ni, Al_2O_3, and composites in ferrite-based magnetic materials that can absorb more than 90% of electromagnetic waves in the frequency range 2-18 GHz.

Keywords
$BaFe_{12}O_{19}$, betel leaf, hydrothermal and electromagnetic absorption

Received: 8 December 2020, Accepted: 31 March 2021
https://doi.org/10.26554/sti.2021.6.2.39-52

1. INTRODUCTION

The barium hexaferrite material is a ferrite-based magnetic material that has large magnetic loss properties and dielectric loss properties (Handoko et al., 2020), high magnetization saturation, high conductivity, and high-temperature curie (Kumar et al., 2020). These characteristics make barium hexaferrite a better absorbent material for electromagnetic radiation than other materials (Bahadur et al., 2017). So far barium hexaferrite has only been developed through the formation of compounds and the addition of composite elements such as TiO_2, Al_2O_3 dan $CuCO_2SO_4$ (Peymanfar et al., 2020; Vinnik et al., 2018; Yang et al., 2019).

The development of research on barium hexaferrite material needs to be modified and engineered to obtain appropriate and precise parameters to produce electromagnetic wave absorbing material, for example by adding plant media. According to Guo's research, plants can absorb electromagnetic radiation (Guo et al., 2019). Some researchers have utilized plant extracts in ferrite syntheses such as aloe vera extract and Hisbiscus rosa in nanocrystalline $MnFe_2O_4$ (Manikandan et al., 2015). Other plants such as Pumelo peel, sansevieria trifasciata, and piper betle Linn is reported to be absorbent against electromagnetic waves due to the composition of flavonoids in these plants (Adhityaxena et al., 2020; Liu et al., 2017; Purba, 2019).

This research uses piper betle Linn as an object of media extract in barium hexaferrite based on a literature review. Piper betle Linn is a medicinal plant that has the property of absorbing electromagnetic waves due to its high flavonoid content as an adsorbent compared to other plants (Purba, 2019). Flavonoids are natural phenolic compounds that can adsorb free radicals by donating hydrogen atoms from hydroxyl groups (Ullah et al., 2020). Flavonoid compounds can absorb electromagnetic radiation through hydrophobic interactions, ion exchange, and electrostatic due to electrons undergoing electronic transitions.

With the support of theories, observations, and literature studies conducted on barium hexaferrite and betel leaf as absorbent materials, we are interested in digging deeper into the potential effectiveness of betel leaf in barium hexaferrite as a smart solution to absorb electromagnetic radiation. The pur-

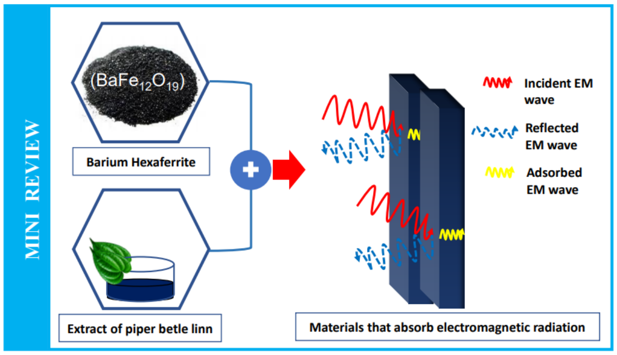

Figure 1. Illustration of this Article's Literature Review On $Bafe_{12}O_{19}$ and Piper Betle Linn

pose of this mini-review is to specifically determine the chemical composition of the betel leaf, the characteristics of the barium hexaferrite material as an absorbent material for electromagnetic radiation, and to analyze possible research methods to synthesize the two materials into one unit with homogeneous properties without reducing the properties and characteristics of both materials.

2. THE DEVELOPMENT OF RESEARCH $BaFe_{12}O_{19}$

Reviewing the progress of research developments that discuss electromagnetic wave adsorption, every year several researchers have succeeded in synthesizing adsorbent materials by considering the composition, materials, and additives in increasing sorbent ability. Several materials such as carbon-based composites (Wu et al., 2021), conductive polymer composites (Song et al., 2021), and nanofiber from electrospinning (Huang et al., 2020) have been successfully developed to absorb microwave or electromagnetism. One material that has caught our attention is $BaFe_{12}O_{19}$, this material has been studied to have high coercitivity, high anisotropy, and high permeability, which meet the criteria as a material or device that absorbs micro and electromagnetic radiation (Zhu et al., 2020). Table 1 shows the development of research on barium hexaferrite magnets as a material with the ability to absorb electromagnetic radiation. Various methods have been researched and resulted in different reflection loss values. In this review, we are interested in discussing additional materials in the form of media extracts in magnetic materials to determine their potential and effectiveness in improving the function or characteristics of magnets, as illustrated in Figure 1.

3. COMPOSITION AND CHEMICAL CHARACTERISTICS OF PIPER BETLE LINN

Based on the literature review, the chemical and biological compounds of piper betle Linn are as shown in Table 2. Piper betle Linn contains more essential oil compounds. (Madhumita et al., 2019), phenolic acid, antioxidants, and high flavonoids can help in the process of material synthesis (Punuri et al., 2012). Piper betle Linn also contains high antioxidants (Tagrida and Benjakul, 2020) alkaloids, steroids, tannins, saponins, and amino acids that can inhibit the electron transport system. The chemical composition includes the phenol group with the most flavonoid compounds. Flavonoid compounds have hydroxyl and superoxide scavenging groups that can be used to remove radioactive components from the air (Madhumita et al., 2020). The darker color of the betel leaf extract, the higher the levels of flavonoids contained. This is due to the high levels of flavonoids so that the molecules contained in the betel leaf extract are increasing and can absorb a certain wavelength in increasing numbers (Saryanti et al., 2020).

In recent years betel leaf extract has been researched and successfully synthesized in Fe_2O_3 and silver and gold nanoparticles as a reducing agent and stabilizer of material synthesis (Shejawal et al., 2020). Piper betel Linn can absorb air pollutant particles from formaldehyde and benzene compounds (Sadishkumar and Jeevaratnam, 2016). Atiya conducted a cell culture study for anticancer activity isolated from chloroform extract of Piper betle Linn leaves as cytotoxic activity against human oral cancer cell lines (Atiya, 2017), Misra et al., 2018 conducted research on betel leaf modified with super magnetic iron oxide as a magnetic nano sorbent to remove drugs from aqueous solutions such as carbamazepine. Piper betle can effectively and efficiently catalyze the degradation of a substance in the photocatalytic process (Misra et al., 2018). Kaur et al., 2020 successfully synthesized TiO_2 nanoparticles (NPs) and SnO_2 nanoparticles mediated by Piper betle with the green synthesis method for the reduction of industrial reactive yellow-86 dye and yellow 186 dye under direct sunlight under optimal conditions (Kaur et al., 2020).

Raja and Sundaramurthy, 2021 conducted a study of green synthesis of fluorescence carbon quantum dots from piper betle via hydrothermal method. The synthesized betel leaf extract has selective characteristics that can detect Fe^{3+} in aqueous media in the presence of other metal ions such as (Ca^{2+}, Cu^{2+}, Mg^{2+}, Ag^{+}, Hg^{2+}, Fe^{2+}, Fe^{3+}, Cd^{2+} dan Pb^{2+}) at the same concentration and is also very sensitive to detect 50–150 nM concentration with coefficient co-relation value (R^2) = 0.9944 (Raja and Sundaramurthy, 2021). Based on research conducted by (Saryanti et al., 2020), nanoparticles can accelerate mass transfer and increase the antibacterial and antioxidant activity of betel leaf so that it has the potential to increase drug absorption and effectiveness.

Based on the results of several literature studies, a betel leaf is a plant that can absorb a compound, substance, or radiation due to the content of flavonoid compounds in it. This paper will examine the use of betel leaf as a medium for extracting electromagnetic radiation. To determine the effectiveness of betel leaves in absorbing electromagnetic radiation, the leaves can be applied in barium hexaferrite magnet material because of their chemical compounds which can help in the process of material synthesis. (Punuri et al., 2012) with a stable material nanoparticle yield (Raj et al., 2012).

4. MODIFICATION OF MATERIAL DEVELOPMENT FOR BARIUM HEXAFERRITE AND PIPER BETLE LINN

Several plant extracts have been used in several studies to synthesized clean nanoparticles, such as alfalfa, aloe vera, turmeric,

Table 1. The State of the Art Barium Hexaferrite Material with Additional Material to the Reflection Loss Value

Magnetic Sample	Methode of Synthesis	Reflection Loss dB (range)	References
Polyaniline/$BaFe_{12}O_{19}$	in situ polymerization	-10 dB	(Ting and Wu, 2010)
E^{3+}/barium ferrite	polymer adsorbent combustion	-10 dB	(Huang et al., 2010)
Dy^{3+}/barium ferrite	solid-state	-15 dB	(Wang et al., 2011)
$BaFe_{12}O_{19}$ + $BaTiO_3$	in situ polymerization	-10 dB	(Yang et al., 2011)
$BaFe_{12}O_{19}$/ZnO	sol-gel and co-precipitation	-37.5 (13.7–18.0 GHz)	(Chen et al., 2012)
$BaFe_{12}O_{19}$/ $Ni_{0.8}Zn_{0.2}Fe_2O_4$	sol-gel	-21.5 dB (2-15 GHz)	(Yang et al., 2011)
$BaFe_{12}O_{19}$ ferrite	microemulsion	-28.52 dB (8–18 GHz)	(Li et al., 2013)
$BaFe_{12}O_{19}$ with Novolac phenolic resin	precipitate	-24.61 (8.2-12.4 GHz)	(Ozah and Bhattacharyya, 2013)
$BaFe_{12}O_{19}$/Nano graphite	magnetoplumbite ferrite	-17.06 dB at (9.27 GHz)	(Yang and Wang, 2014)
$(Mn_{0.2}Ni_{0.4}Zn_{0.4}Fe_2O_4)$/ $(BaFe_{12}O_{19})$	one-pot	-25 dB at (-8.2 GHz)	(Hazra et al., 2014)
graphene/$BaFe_{12}O_{19}$/ $CoFe_2O_4$	deoxidation	-32.4 dB (2–18 GHz)	(Yang et al., 2015)
$BaFe_{12}O_{19}$/$CoFe_2O_4$	in situ	-10 dB (8.2–16.3 GHz)	(Huang et al., 2015)
graphene/0.8$BaFe_{12}O_{19}$/ 0.2$Y_3Fe_5O_{12}$	deoxidation	-41.5 (4.6–8.2 GHz)	(Lin et al., 2016)
barium hexaferrite/ calcium titanate	hydrothermal	-34 dB at 9.8 GHz	(Afghahi et al., 2016)
graphene aerogel (GA)/ $BaFe_{12}O_{19}$	self-propagating combustion	-10 dB (2–18 GHz)	(Zhao et al., 2017)
$BaFe_{12}O_{19}$ nano ferrite	co-precipitation	-26.52 dB at 5.79 GHz	(Bahadur et al., 2017)
RGO/$BaFe_{12}O_{19}$/Fe_3O_4	solvothermal	-46.04 dB at 15.6 GHz	(Jiao et al., 2018)
(Gd, Mn, Co) $BaFe_{12}O_{19}$	hydrothermal	-47 dB at 17.2 GHz	(Torabi et al., 2017)
$BaFe_{12}O_{19}$@Carbon	hydrothermal	-73.42 dB (2-8 GHz)	(Liu et al., 2019)
$BaFe_{12}O_{19}$/ $La_{0.5}Sr_{0.5}MnO_3$	complementary citrate gel and ultrasonic	-67.10 dB at 11.6 GHz	(Peymanfar et al., 2019)
$BaFe_{12}O_{19}$ graphene oxide	uto-combustion reaction	-52.21 dB at 10.72 GHz	(Goel et al., 2020)
$BaFe_{12}O_{19}$@MoS_2	hydrothermal	-61 dB at 4.4 GHz	(Wang et al., 2020)
$BaFe_{12}O_{19}$@MnO_2	hydrothermal	-54.39 dB at 4.64 GHz	(Hu et al., 2021)
PANI/$BaFe_{12}O_{19}$@Halloysite	sol-gel	-14.77 dB at 11.92 GHz	(Chen et al., 2021)

Table 2. Table Review Chemical Composition of Betel Leaf

Piper Betle Leaves Extract	Chemichal Composition	Reference
Review: Betel leaf extract powder using Soxhlet apparatus with 70% deionized water and ethanol	Alkaloids, fatty acids, phenolic compounds, alcoholic compounds, flavonoids compounds, terpenes compounds, coumarin compounds, and organic acids.	(Madhumita et al., 2020)
Betel leaf extract, distilled water, 70% alcohol, and antibiotics.	The essential oil contains hydroxy cyclic compounds, kavikol, cavibetol, estradiol, eugenol, metaleugenol, carvacrol, terpeneba, sesquiterpene, phenyl propane, and tannins.	(Elfrida et al., 2020)
Antioxidant and antimicrobial potential of selected varieties of Piper betle L. (Betel leaf)	Hydroxychavicol, chavicol, piper betel, cavibetol, piperol A, methylpiperbetol, piperol, and volatile oil.	(Sarma et al., 2018)

Capsicum annuum, geranium, coriander, tea, and neem (Thakur et al., 2020). Barium hexaferrite material with plant modification can increase the absorption of electromagnetic radiation, because of the nature of $BaFe_{12}O_{19}$ which is easily synthesized with natural ingredients (Gu et al., 2019). The mixing of the two ingredients between the barium hexaferrite precursor and betel leaf extract can be done using a microemulsion method Koutzarova et al., 2013, solid-state, coprecipitation Alonso-Rodríguez et al., 2020, sol-gel Mosleh et al., 2016 and hydrothermal synthesis (Zhao et al., 2013). In general, the things that need to be considered in some of these methods are the percentage of the mixture of materials, the calcination process, compaction, and sintering (Rusianto et al., 2015). A literature review of synthesis methods with the addition of plant extracts and compounds to ferrite-based magnets can be seen in Table 3.

The microemulsion method stabilizes the two mixtures with the surfactant molecules used (Foroughi et al., 2015) with the results of uniform particle size by varying the properties of the surfactant, co-surfactant (Hasany et al., 2013). The synthesis of barium hexaferrite using the co-precipitation method is a technique that is often applied in the manufacture of ferrite-based magnets with the results of the size of the nanoparticles (Li et al., 2015). Barium hexaferrite with high saturation magnetization was synthesized using the sol-gel method showing a total shielding effectiveness value in absorbing radiation above 20 dB with a maximum total shielding effectiveness value of 31.97 dB at 10.30 GHz with a thickness of 2 mm Carol et al., 2020 however the resulting ferrite nanoparticles are less pure due to contamination from the reaction byproducts (Kefeni et al., 2017). The solid-state reaction method involves heating a mixture of oxide and barium carbonate powder to produce the desired phase at low raw material costs and a simple process (Fan et al., 2020). In this case, hydrothermal synthesis is very suitable as a method that combines plant extracts with ferrite-based magnetic materials based on the results of the literature review in Table 3.

5. HYDROTHERMAL SYNTHESIS

Based on the development of research on ferrite-based magnetic synthesis methods, One method that has succeeded in synthesizing betel leaf as a medium in barium hexaferrite magnets is a hydrothermal synthesis method with a good level of homogeneity without reducing the characteristics of the two materials (Rahmayeni et al., 2020). Hydrothermal synthesis involving the green synthesis method has been widely researched and succeeded in producing magnetic nanoparticles with plant extracts. Ramasahayam et al., 2012 synthesized magnetic nanocomposites using pine wood shavings (Ramasahayam et al., 2012). Iron oxide nanorods have been previously studied by López-Téllez et al., 2013 using bark extracts. The content of chemical compounds in orange peels such as starch, cellulose, hemicellulose, and lignin acts as a stabilizer by reducing Fe(II) metal ions. According to their research, Fe is deposited on the surface of the biomass and is mostly present in the form of Fe, Fe_2O_3, and magnetite(López-Téllez et al., 2013). Several other plant extracts have also been successfully synthesized with ferrite-based magnets or by using the green synthesis hydrothermal method. For example rhizome extract of Acorus Calamus Thakur et al., 2020, extract of green tea (Hebbalalu et al., 2013), Piper betle Linn Rahmayeni

Table 3. Table Review of the Synthesis Method of Ferrite with the Addition Compounds

Substitution/ Plant Extracts	Methode of Synthesis	Review of Results	Reference
$BaFe_{12}O_{19}$ with rhizome extract of Acorus Calamus.	Green Synthesis (Hydrothermal)	XRD shows the magnetic structure without any impurities. SEM showed the synthesized solid packaging of BFNP and its uniform distribution. Green technology has the potential to produce magnetic nanoparticles.	(Thakur et al., 2020)
Green tea extracts with AgNPs	Green Synthesis (Hydrothermal)	The AgNP produced is non-toxic to humans and does not damage the surface of the material. Plant extract can reduce the size of silver particles	(Hebbalalu et al., 2013)
Extract piper betle leaf with $MnFe_2O_4$	Green Synthesis (Hydrothermal)	SEM shows that the resulting magnet has a homogeneous surface structure. XRD shows the size of the ferrite particles on the nanometer scale.	(Rahmayeni et al., 2020)
$CoFe_2O_4$–carbon quantum dots nanocomposite by turmeric	Green Synthesis (Hydrothermal)	XRD results show that the crystal structure of $CoFe_2O_4$ by turmeric matches the crystal structure of pure $CoFe_2O_4$. The addition of turmeric to magnets does not damage the magnetic properties and has the potential as a photocatalytic activity	(Ahmadian-Fard-Fini et al., 2017)
Urtica plant extract with $NiFe_2O_4$	Green Synthesis (Hydrothermal)	No phase or other impurities were detected in the pattern obtained from XRD with nanometer crystal size, hydrothermal synthesis reduces material agglomeration	(Amiri et al., 2018)
$NiFe_2O_4$ with almond	Green Synthesis (Hydrothermal)	The hysteresis curve of $NiFe_2O_4$ carbon nanocomposites shows ferromagnetic properties. The magnetic nanostructures exhibit suitable magnetization, which can be easily attracted by magnets.	(Ahmadian-Fard-Fini et al., 2019)
Mn-Zn Ferrite with oxide NP	Microemulsion	There was a decrease in the microemulsion area that overlaps with the precursors	(Kumar et al., 2018)
$BaFe_{12}O_{19}$ with Ni^{2+}	Solid-state	XRD shows the impurity phase formation in pure $BaFe_{12}O_{19}$ samples, SEM shows anisotropy, and the mean particle size increases.	(Rafiq et al., 2016)
Piper betle with superparamagnetic iron oxide	Coprecipitation	XRD confirmed the magnetic crystal size in the nanometer scale (20 nm), the adsorption value was lower than the Nelumbo nucifera plant by this method.	(Misra et al., 2018)
$BaFe_{12}O_{19}$ with polyaniline composite	Coprecipitation	Magnets have the potential to act as adsorbing materials against electromagnetic interference	(Meng et al., 2019)

Table 4. Effect of Calcination Concentration and Temperature On Material Homogeneity (Rahmayeni et al., 2020)

Comparison of Ferrite Volume and Betel Leaf Extract	Calcination Temperature Treatment	Particle Size Distribution	Homogeneity Level
47:03:00	-	133	not good
47:03:00	500°C	167	not good
47:05:00	-	90	good
47:05:00	500°C	120	not good

Table 5. Magnetic Properties $BaFe_{12}O_{19}$

Sample	Size Particle	Ms	Hc (Oe)	Range freq. (GHz)	Absorption Freq. (GHz)	RL (dB)	References
$BaCo_{0.5}Cu_{0.5}ZrFe_{10}O_{19}$	50-500	49.07	396.91	Dec-18	14.4	27.4	(Nikmanesh et al., 2019)
$BaFe_{12}O_{19}$ NPs	78	75.54	207.3	Feb-18	5.79	26.5	(Bahadur et al., 2017)
$BaFe_{12-x}Ni_xO_{19}$	1.4147	57.57	1240.6	-	-	-	(Rafiq et al., 2016)
$BaFe_{12}O_{19}$@polyaniline composite	500	-	-	Feb-18	7.24	25.6	(Misra et al., 2018)
$BaFe_{12}O_{19}/NiFe_2O_4$	30	55.188	-	9-Dec	11.79	27.1	(Meng et al., 2019)
$BaFe_{12}O_{19}$	-	34.2	2000		37.6	20	(Li et al., 2016)

et al., 2020, turmeric, almond (Ahmadian-Fard-Fini et al., 2019; Ahmadian-Fard-Fini et al., 2017) and extract Urtica Sharifi et al., 2012, the homogeneous level of mixing the two materials can be seen in Table 3.

Leaf extract is used as a bioreduction and capping agent to produce magnetic nanoparticles from the Fe_3O_4 solution. Nanoparticles are obtained by separation from solution (Madhubala and Kalaivani, 2018; Prasad et al., 2017). The hydrothermal synthesis method is one of the most promising synthesis methods for the large-scale production of ferrite-based nanoparticles. Hydrothermal synthesis is a single crystal synthesis method that relies on the solubility of minerals in hot water and under high pressure (Pan et al., 2015). Hydrothermal synthesis is influenced by the type of solvent, temperature, and duration of synthesis. This method uses a solvent with a higher moisture content to help precipitate the larger ferrite magnet particles. In the formation of ferrite particles, hydrothermal synthesis undergoes a process of nucleation and grain growth, whose production rate is controlled by temperature. At higher temperatures, the nucleation becomes faster than grain growth so that the particle size decreases, but if the reaction duration is extended, grain growth will be advantageous in the reaction (Fu and Ravindra, 2012). Hydrothermal synthesis has advantages over other methods such as relatively low cost, non-toxic, environmentally friendly precursors, and simple procedures. The formation of good quality nanoparticles with controlled size and size distribution can be achieved by selecting the appropriate solvent mixture and various parameters such as temperature, pressure, and reaction time (Saryanti et al., 2020).

The green hydrothermal synthesis process has been researched by Ahmadian-Fard-Fini et al., 2018 in mixing ferrite-based mag-

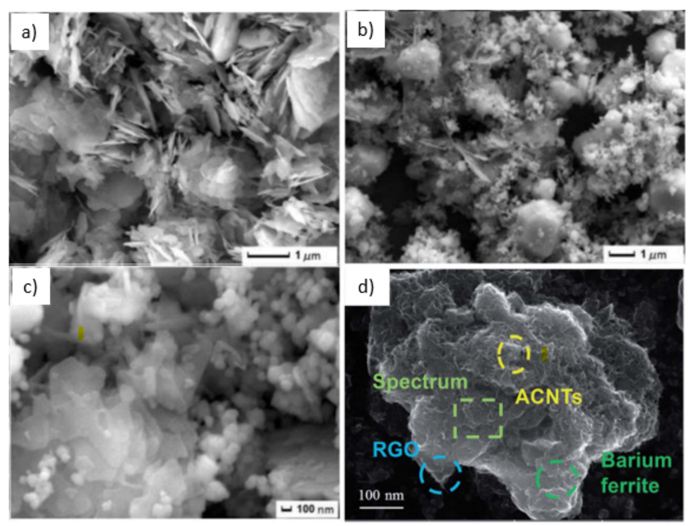

Figure 2. Results of Characterization of Ferrite Material Morphology with the Scanning Electron Microscope (SEM) (a) Pure $BaFe_{12}O_{19}$, (b) 10% $BaFe_{12}O_{19}/Ag_3PO_4$ Composite Material in the Low Magnification, (c) High Magnification Adapted from Xu et al., 2019 with Permission from Royal Society Chemistry, (d) Barium Hexaferrite with the Addition of ACNT/RGO, Adapted from Zhao et al., 2017 with Permission Royal Society Chemistry

nets (Fe_3O_4) with lemon and grape extract. The research used 50 mL of solvent at high nucleation pressures in a Teflon-lined stainless autoclave. The process is carried out at 180°C for 6 hours to produce a particle distribution on the nanometer scale. Based on the research conducted by Rahmayeni in synthesizing betel leaf media extract and ferrite-based magnetic material with the synthesized hydrothermal method, a final material with a good homogeneity level was obtained through observations of morphological studies. The morphology of $BaFe_{12}O_{19}$ is an irregular flaky structure (Figure 2a). The results of Xu et al., 2019 research shows that the image of barium hexaferrite SEM samples with the addition of a 10% Ag_3PO_4 composite can reduce the size of the spherical magnet at low-magnification (Figure 2b). In the high-magnification SEM images, the tiny spherical particles were successfully attached to the $BaFe_{12}O_{19}$ sample, illustrating their combined structure (Figure 2c). On other hand, also shows that the $Bafe_{12}O_{19}$ sample is a solid polycrystalline (> 98%) (Matzui et al., 2019). Besides, the research that has been done by Zhao et al., 2017 (Figure 2d) shows a high magnification SEM image of amorphous carbon nanotubes (ACNT) / reduced graphene oxide (RGO) / Barium hexaferrite. The addition of ACNT and RGO is evenly distributed and homogeneous at the reaction time and forms a conductive network structure that is interlinked in the BF magnet, which can increase the dielectric loss of the composite.

The addition of piper betle Linn extract as media extract in Manganese Ferrite magnet material has been previously done by Rahmayeni et al., 2020, with a variety of compositions. The morphology of using betel leaf media extract with a volume ratio of 45: 5 to produce fine, homogeneous, and uniform particles of cubic crystal structure were analyzed using a Scanning Electron Microscope (SEM). A more detailed analysis of the morphology and crystallinity of manganese ferrite which is the result of the Transmission Electron Microscope (TEM) characterization, the shape of the cubic particles according to the SEM image results. Morphological properties and material magnetic crystallization are influenced by betel leaf concentration and calcination temperature as shown in Table 4. Comparison of the volume composition of the magnetic solution with the best media extract in producing homogeneous particles is 45: 5 without calcination temperature treatment. The calcination process causes the growth of particles, resulting in larger but non-uniform particles (Rahmayeni et al., 2020). As shown in Figure 3, based on the results of the study Yin et al., 2015, the edges of the catalyst particle lattice can be seen clearly, with the accurate measurement of the HRTEM image of the catalyst particles, TEM characterization results were also obtained which confirmed the morphological suitability of the samples in SEM. It can be observed that a straight CNT has a quasi-linear structure with an outer diameter and an inner diameter ranging from 75–95 nm and 25–45 nm (Yin et al., 2015).

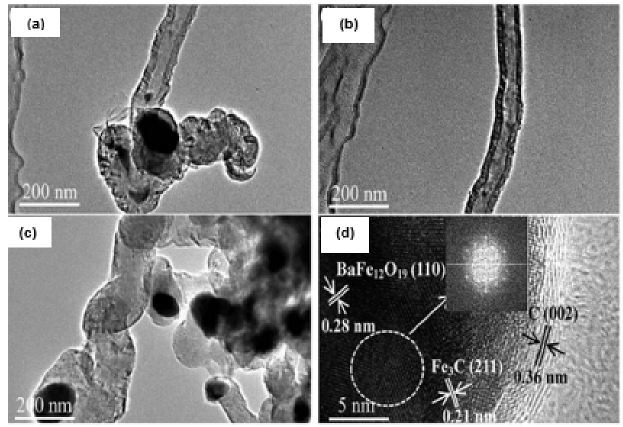

Figure 3. TEM Images of $Bafe_{12}O_{19}/Fe_3C$/Cnts Composites Synthesized at 600°C Adapted from Yin et al., 2015 with Permission Royal Society Chemistry

6. CHARACTERISTICS OF $BaFe_{12}O_{19}$ AS AN ABSORPTION OF ELECTROMAGNETIC WAVES

Barium hexaferrite is an ideal magnet for microwave absorbers due to its magnetization and high anisotropy field as well as good chemical stability. The natural ferrimagnetic resonance frequency of this material is about 50 GHz, due to its large magnetocrystalline anisotropy (Sözeri et al., 2015). The structure, phase purity, and size of the magnetic crystals were confirmed by analyzing powder X-ray diffraction (XRD). One of the $BaFe_{12}O_{19}$ crystallographic information obtained from the XRD pattern results of Marouoai's research is shown in Figure 4. All major peaks in the diffraction pattern can be indexed to various planes (hkl) $BaFe_{12}O_{19}$ which matches perfectly with the hexagonal structure of pure $BaFe_{12}O_{19}$, which states that adding media to $BaFe_{12}O_{19}$ magnets does not damage the crystal structure (Marouani et al., 2021).

Calcination temperature treatment in the synthesis process of barium hexaferrite also affects the crystallinity of the sample. Rahmayeni et al., 2020 research results also show the crystal structure of a ferrite-based magnet mixed with betel leaf media extracts without calcination temperature. The 45: 5 composition indicated by the MnE5N compound states that no Fe_2O_3 impurities were observed. It can be concluded that the amount of betel leaf extract used affects the structure of manganese ferrite. MnE5N states the compound ratio of the composition of the ferrite-based magnetic solution to the 45: 5 media extract solution with a cubic crystal structure with a more even particle size distribution compared to MnE3N and MnE1N. So that betel leaf extract in magnetic materials has been studied and reviewed that it does not damage the surface morphology, crystal structure, and particle size of the magnetic material used (Rahmayeni et al., 2020).

The magnetic properties of barium hexaferrite were measured using a Vibrating Sample Magnetometer (VSM) as illustrated in Figure 5 and Table 5. Table 5 shows the results of studies where $BaFe_{12}O_{19}$ was substituted with ions or other materials.

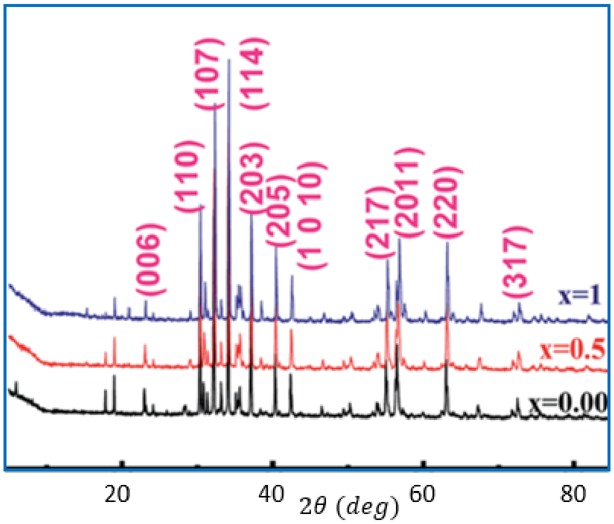

Figure 4. Illustration of the X-Ray Diffraction Pattern of Barium Hexaferrite with Added Strontium, Adapted from Marouani et al., 2021 with Permission Royal Society Chemistry

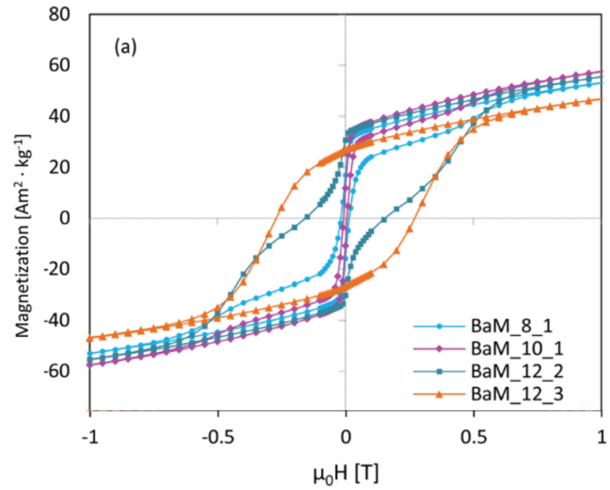

Figure 5. Parts of Magnetic Hysteresis Loops for Selected $BaFe_{12}O_{19}$ Samples Obtained within Fe^{3+}/Ba^{2+} (Hysteresis Curve of VSM Output) Adapted from Dudziak et al., 2020 with Permission Royal Society Chemistry

The addition of media extract can increase the reflection loss (RL) value of the magnet. $BaFe_{12}O_{19}$ magnetic properties are shown by the hysteresis curve in Figure 5. In general, the magnetization saturation (MS) value of the barium hexaferrite magnet obtained from the research results by Dudziak ranged from 58-68 Am^2 kg^{-1}. For some samples, values very close to the theoretical value of 72 Am^2 kg^{-1}. In all series, the highest magnetization was observed for single-phase $BaFe_{12}O_{19}$ samples, because both $BaFe_2O_4$ and Fe_2O_3, occurring as impurities, have no or weak ferromagnetic properties (Dudziak et al., 2020). Based on conducted Nikmanesh et al., 2019 with different levels of doping material concentration. From the hysteresis curve, the values of magnetic properties are obtained in the form of magnetic saturation (Ms), remittance (Mr), coercitivity (Hc), maximum energy production temperature curie and the effective average anisotropy constant.

Based on research conducted by Ovalioglu et al., 2010, the characteristics of barium hexaferrite magnets can be widely used as permanent magnets because the magnetocrystalline anisotropy (K_1) is quite large at 77K and high curie temperatures, with relatively large saturation magnetization, good chemical stability, and resistance. corrosion (Ovalioglu et al., 2010). $BaFe_{12}O_{19}$ shows dielectric properties with a conductivity value of 10^{-2} S/cm Vinnik et al., 2020 and has a large number of atomic magnetic fields due to the spin magnetic moment of unpaired free electrons (Xu et al., 2019). Magnetic fields can also affect the current efficiency, layer particle content, surface morphology, and coating properties of the material (Setiamukti et al., 2020). Crystallite size (D) is the most important factor for the coercivity (Hc) value. Materials with fine structure and in the order of nanometers affect the value of Hc by Equation 1 following:

$$Hc = Pc\frac{K_1^4 D^6}{MsA} \quad (1)$$

Where pc, K_1, and A show the dimensionless factor, exchange stiffness, and effective mean anisotropy constant, respectively. The smaller the crystal size in the nanometer scale, the smaller the magnetic coercitivity value (Li et al., 2016). Based on the results of a literature review regarding the use of betel leaf media extract in ferrite-based magnetic materials, it does not change and damage the magnetic properties of the material.

7. EFFECTIVENESS OF MEDIA EXTRACT IN $BaFe_{12}O_{19}$ AS ELECTROMAGNETIC WAVE ABSORPTION

The identification of the amount of material absorption to electromagnetic waves is analyzed using the Vector Network Analyzer (VNA) method. The results of Barium Hexaferrite characterization using the VNA method by results (Zhao et al., 2017) are shown in Figure 6. Furthermore, the intertwined structure consists of ACNT and graphene sheets which intertwine spontaneously and respond intensely to broadband incident waves. It comes as an excellent resistance-inductance-capacitance coupled circuit. The interaction of electromagnetic waves with dielectric materials strengthens molecular motions such as ionic conduction, dipolar polarization (Zhao et al., 2017). Other research shows $BaFe_{12}O_{19}$ Reflection Loss below -5 dB, microwave absorption >70%. Compared to pure $BaFe_{12}O_{19}$, added dopping increases to higher frequencies for BSFO, BCFO, BFCO, and BFMO. The best absorption was obtained for BCFO and BFMO ceramics with the same RLmin -18.5 dB at 6.7 and 7.2 GHz, RL bandwidth below -5 dB of 5.5–9.1, and 3.6–18 GHz. $BaFe_{12}O_{19}$ can absorb a frequency of 7.24 GHz in the 2-18 GHz range. The

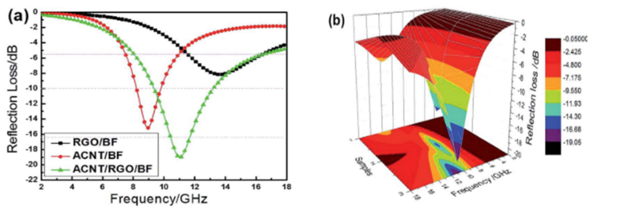

Figure 6. The Electromagnetic Wave Absorbing Properties of ACNT/RGO/BF, RGO/BF, and ACNT/BF Composites (a) Two-Dimension, (b) Three-Dimension, Adapted from Zhao et al., 2017 with Permission Royal Society Chemistry

highest reflection loss value shows several 25.6 dB, so the addition of other elements or media in $BaFe_{12}O_{19}$ can increase the material's ability to absorb electromagnetic waves (Meng et al., 2019).

The permittivity and permeability are used for the characterization of dielectric constant and magnetic loss properties of the electromagnetic wave absorbing materials. In Figure 7 (a and b), the dielectric constant 30 decreases slightly with increasing frequency. According to the Koops theory based on the Maxwell Wagner model for an inhomogeneous double layer dielectric structure, the conductive grains of wells in iron crystals are separated by poorly conductive grain boundaries. At low frequencies, grain boundaries are more effective than conductive grains. Due to the high resistance of the grain boundaries, the jumping electrons will accumulate and produce polarization in this area. High electronic conduction at low frequencies due to polarization. The trend of the lines in Figure 7 (c and d) is similar because the carbon nanomaterial has poor magnetic loss and all the lines show $BaFe_{12}O_{19}$ properties. The significant difference in permeability between RGO / BF, ACNT / BF, and ACNT / RGO / BF in 2–5 GHz may be due to the different ACNT content in these three composites. There may be a residual catalyst in the ACNT, which can cause magnetic loss and affect the actual permeability (Zhao et al., 2017).

The ε' of samples vary gradually and their ε" is close to zero, suggesting the weak dielectric loss of the nanocomposite. The value of μ' remain nearly constant for low content samples and show no significant variation with frequency and then the real part of permeability increase. Value of μ" increases with increasing substitution (Nikmanesh et al., 2019). The addition of media extract can increase the permittivity and permeability value of $BaFe_{12}O_{19}$. When microwaves hit material with an electromagnetic absorbent material it will form an electric field on the surface of the absorbent, after which the current flows as a surface current (Susilawati et al., 2017). Absorption materials, in general, can absorb electromagnetic waves by absorbing the power that penetrates the material and then converting them into heat energy. The results of the analysis of ferrite sample absorption with media extracts against electromagnetic waves in the 2-18 GHz range can be more than 90% (Liu et al., 2019). This states that the emission of electromagnetic waves is absorbed

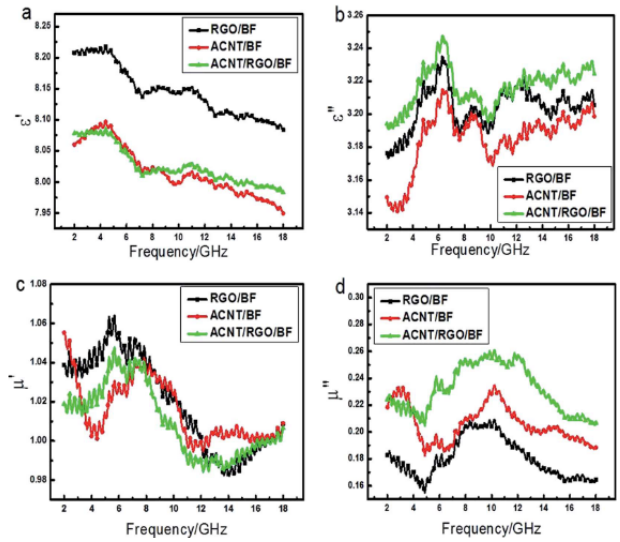

Figure 7. Electromagnetic Properties of ACNT/RGO/BF, RGO/BF, And ACNT/BF Composites Vs. Frequency. (a and b) the Complex Permittivity (ε', ε"); (c and d) the Complex Permeability (μ', μ") Adapted from Zhao et al., 2017 with Permission Royal Society Chemistry

more by the material than the electromagnetic waves that are reflected by the magnetic surface (Luthfianti et al., 2020).

8. CONCLUSION

This mini-review comprehensively focuses on the development aspects of $BaFe_{12}O_{19}$ magnet research and betel leaf as an absorbent material for electromagnetic radiation. Based on the innovation of the results of this literature, it is hoped that there will be an integration of research developed using other materials, given the abundant natural potential of Indonesia. Research that discusses modifications to increase the adsorption power of $BaFe_{12}O_{19}$ against electromagnetic radiation, always develops every year, we believe, the topics we discussed in this mini-review will start to grow and hopefully continue to develop for newness in the field of research or science.

Piper betel Linn has the potential to increase the effectiveness of magnetic absorption in absorbing electromagnetic waves. The effectiveness of betel leaf extract in the synthesis of barium hexaferrite material can reach 90% over the 4-18 GHz range. Betel leaf has flavonoid chemical compounds that have hydroxyl and superoxide scavenging groups which can be used to remove radioactive components from the air. The darker the color of the betel leaf extract, the higher the levels of flavonoids contained and the greater the amount of electromagnetic radiation that is absorbed. So far, the methods of microemulsion, solid-state, coprecipitation, sol-gel, and hydrothermal synthesis are methods that can synthesize betel leaf as a media extract in barium hexaferrite. The hydrothermal synthesis method is the best method that can synthesize barium hexaferrite and betel leaf precursors with better homogeneity and particle size distribution on the nanometer scale based on literature studies. Mixing betel leaf media extract in a magnetic material has been studied, the conclusion is that the betel leaf in the media extract does not damage the surface morphology, crystal structure, and particle size of the magnet without reducing the magnetic characteristics of the material.

We recommend carrying out laboratory studies in developing the composition of the betel leaf extract media and barium hexaferrite solution to be more varied in volumes greater than 50 mL. The author also hopes that the media extract of betel leaf (Piper betle Linn) can be compared with red betel leaf (Piper Crocatum) to test its effectiveness in barium hexaferrite as an electromagnetic wave absorbing material.

9. ACKNOWLEDGMENT

This research was funded by the Learning and Student Affairs Information System (SIMBELMAWA) Ministry of Education and Culture, the Republic of Indonesia in 2020 with contract number 042 / E2 / PPK / SPPK / PKM-B2 / 2020. Therefore, we thank you for the support and assistance that has been given. We also express our gratitude to Sriwijaya University, supervisors, and reviewer colleagues who have helped, motivated, and provided valuable suggestions and input.

REFERENCES

Adhityaxena, A. T., A. Megantika, R. Arbianti, T. S. Utami, and H. Hermansyah (2020). Extraction of Flavonoid from Mother-in-law's Tongue Leaves (Sansevieria trifasciata) by Ultrasound Assisted Enzymatic Extraction and its Inhibition Test. In *International Conference On Trends In Materials Science And Inventive Materials: ICTMIM 2020*. AIP Publishing

Afghahi, S. S. S., M. Jafarian, and Y. Atassi (2016). A promising lightweight multicomponent microwave absorber based on doped barium hexaferrite/calcium titanate/multiwalled carbon nanotubes. *Journal of Nanoparticle Research*, **18**(7)

Ahmadian-Fard-Fini, S., D. Ghanbari, and M. Salavati-Niasari (2019). Photoluminescence carbon dot as a sensor for detecting of Pseudomonas aeruginosa bacteria: Hydrothermal synthesis of magnetic hollow NiFe2O4-carbon dots nanocomposite material. *Composites Part B: Engineering*, **161**; 564–577

Ahmadian-Fard-Fini, S., M. Salavati-Niasari, and D. Ghanbari (2018). Hydrothermal green synthesis of magnetic Fe3O4-carbon dots by lemon and grape fruit extracts and as a photoluminescence sensor for detecting of E. coli bacteria. *Spectrochimica Acta Part A: Molecular and Biomolecular Spectroscopy*, **203**; 481–493

Ahmadian-Fard-Fini, S., M. Salavati-Niasari, and H. Safardoust-Hojaghan (2017). Hydrothermal green synthesis and photocatalytic activity of magnetic CoFe2O4–carbon quantum dots nanocomposite by turmeric precursor. *Journal of Materials Science: Materials in Electronics*, **28**(21); 16205–16214

Alonso-Rodríguez, D., H. Ruiz-Luna, M. Alfaro-Cruz, A. Bañuelos-Frias, L. Alvarado-Perea, and C. Valero-Luna (2020). Synthesis and characterization of BaFe12O19-WC catalysts prepared by mechanical milling. *Fuel*, **280**; 118608

Amiri, M., A. Pardakhti, M. Ahmadi-Zeidabadi, A. Akbari, and M. Salavati-Niasari (2018). Magnetic nickel ferrite nanoparticles: green synthesis by Urtica and therapeutic effect of frequency magnetic field on creating cytotoxic response in neural cell lines. *Colloids and Surfaces B: Biointerfaces*, **172**; 244–253

Atiya, A. (2017). A Novel Resorcinol Derivative from the Leaves of Piper betle. *Chemistry of Natural Compounds*, **53**(4); 611–613

Bahadur, A., A. Saeed, S. Iqbal, M. Shoaib, I. Ahmad, M. S. ur Rahman, M. I. Bashir, M. Yaseen, and W. Hussain (2017). Morphological and magnetic properties of BaFe 12 O 19 nanoferrite: A promising microwave absorbing material. *Ceramics International*, **43**(9); 7346–7350

Carol, T. T. T., J. Mohammed, D. Basandrai, S. K. Godara, G. R. Bhadu, S. Mishra, N. Aggarwal, S. Narang, and A. Srivastava (2020). X-band shielding of electromagnetic interference (EMI) by Co2Y barium hexaferrite, bismuth copper titanate (BCTO), and polyaniline (PANI) composite. *Journal of Magnetism and Magnetic Materials*, **501**; 166433

Chen, W., J. Zheng, and Y. Li (2012). Synthesis and electromagnetic characteristics of BaFe12O19/ZnO composite material. *Journal of Alloys and Compounds*, **513**; 420–424

Chen, Z., D. Mu, T. Liu, Z. He, Y. Zhang, H. Yang, and J. Ouyang (2021). PANI/BaFe12O19@Halloysite ternary composites as novel microwave absorbent. *Journal of Colloid and Interface Science*, **582**; 137–148

Dudziak, S., Z. Ryżyńska, Z. Bielan, J. Ryl, T. Klimczuk, and A. Zielinska-Jurek (2020). Pseudo-superparamagnetic behaviour of barium hexaferrite particles. *RSC Advances*, **10**(32); 18784–18796

Elfrida, E., E. Junaida, R. N. Ariska, and S. Jayanthi (2020). Effect of Piper Betle Linn Extract on the Growth of Staphylococcus Aureus Atcc 25923. *Budapest International Research and Critics Institute (BIRCI-Journal): Humanities and Social Sciences*, **3**(4); 3028–3034

Fan, L., H. Zheng, X. Zhou, H. Zhang, Q. Wu, P. Zheng, L. Zheng, and Y. Zhang (2020). A comparative study of microstructure, magnetic, and electromagnetic properties of Zn2W hexaferrite prepared by sol–gel and solid-state reaction methods. *Journal of Sol-Gel Science and Technology*, **96**(3); 604–613

Foroughi, F., S. Hassanzadeh-Tabrizi, J. Amighian, and A. Saffar-Teluri (2015). A designed magnetic CoFe2O4–hydroxyapatite core–shell nanocomposite for Zn(II) removal with high efficiency. *Ceramics International*, **41**(5); 6844–6850

Fu, C. and N. M. Ravindra (2012). Magnetic iron oxide nanoparticles: synthesis and applications. *Bioinspired, Biomimetic and Nanobiomaterials*, **1**(4); 229–244

Goel, S., A. Garg, R. K. Gupta, A. Dubey, N. E. Prasad, and S. Tyagi (2020). Development of RGO/BaFe12O19-based composite medium for improved microwave absorption applications. *Applied Physics A*, **126**(6)

Gu, H., H. Zhang, C. Ma, H. Sun, C. Liu, K. Dai, J. Zhang,

R. Wei, T. Ding, and Z. Guo (2019). Smart strain sensing organic–inorganic hybrid hydrogels with nano barium ferrite as the cross-linker. *Journal of Materials Chemistry C*, **7**(8); 2353–2360

Guo, L., Q.-D. An, Z.-Y. Xiao, S.-R. Zhai, L. Cui, and Z.-C. Li (2019). Performance enhanced electromagnetic wave absorber from controllable modification of natural plant fiber. *RSC Advances*, **9**(29); 16690–16700

Handoko, E., S. Budi, I. Sugihartono, M. A. Marpaung, Z. Jalil, A. Taufiq, and M. Alaydrus (2020). Microwave absorption performance of barium hexaferrite multi-nanolayers. *Materials Express*, **10**(8); 1328–1336

Hasany, S., N. Abdurahman, A. Sunarti, and R. Jose (2013). Magnetic Iron Oxide Nanoparticles: Chemical Synthesis and Applications Review. *Current Nanoscience*, **9**(5); 561–575

Hazra, S., B. K. Ghosh, H. R. Joshi, M. K. Patra, R. K. Jani, S. R. Vadera, and N. N. Ghosh (2014). Development of a novel one-pot synthetic method for the preparation of (Mn0.2Ni0.4Zn0.4Fe2O4)x–(BaFe12O19)1-xnanocomposites and the study of their microwave absorption and magnetic properties. *RSC Adv.*, **4**(86); 45715–45725

Hebbalalu, D., J. Lalley, M. N. Nadagouda, and R. S. Varma (2013). Greener Techniques for the Synthesis of Silver Nanoparticles Using Plant Extracts, Enzymes, Bacteria, Biodegradable Polymers, and Microwaves. *ACS Sustainable Chemistry & Engineering*, **1**(7); 703–712

Hu, F., H. Nan, M. Wang, Y. Lin, H. Yang, Y. Qiu, and B. Wen (2021). Construction of core-shell BaFe12O19@MnO2 composite for effectively enhancing microwave absorption performance. *Ceramics International*

Huang, W., Z. Tong, R. Wang, Z. Liao, Y. Bi, Y. Chen, M. Ma, P. Lyu, and Y. Ma (2020). A review on electrospinning nanofibers in the field of microwave absorption. *Ceramics International*, **46**(17); 26441–26453

Huang, X., J. Zhang, Z. Liu, T. Sang, B. Song, H. Zhu, and C. Wong (2015). Facile preparation and microwave absorption properties of porous hollow BaFe12O19/CoFe2O4 composite microrods. *Journal of Alloys and Compounds*, **648**; 1072–1075

Huang, X., J. Zhang, H. Wang, S. Yan, L. Wang, and Q. Zhang (2010). Er3-substituted W-type barium ferrite: preparation and electromagnetic properties. *Journal of Rare Earths*, **28**(6); 940–943

Jiao, S., M. Wu, X. Yu, H. Hu, Z. Bai, P. Dai, T. Jiang, H. Bi, and G. Li (2018). RGO/BaFe12O19/Fe3O4 nanocomposite as microwave absorbent with lamellar structures and improved polarization interfaces. *Materials Research Bulletin*, **108**; 89–95

Kaur, G., H. Kaur, S. Kumar, V. Verma, H. S. Jhinjer, J. Singh, M. Rawat, P. P. Singh, and S. Al-Rashed (2020). Blooming Approach: One-Pot Biogenic Synthesis of TiO2 Nanoparticles Using Piper Betle for the Degradation of Industrial Reactive Yellow 86 Dye. *Journal of Inorganic and Organometallic Polymers and Materials*, **31**(3); 1111–1119

Kefeni, K. K., T. A. Msagati, and B. B. Mamba (2017). Ferrite nanoparticles: Synthesis, characterisation and applications in electronic device. *Materials Science and Engineering: B*, **215**; 37–55

Koutzarova, T., S. Kolev, C. Ghelev, I. Nedkov, B. Vertruen, R. Cloots, C. Henrist, and A. Zaleski (2013). Differences in the structural and magnetic properties of nanosized barium hexaferrite powders prepared by single and double microemulsion techniques. *Journal of Alloys and Compounds*, **579**; 174–180

Kumar, S., S. Supriya, L. K. Pradhan, R. Pandey, and M. Kar (2020). Grain size effect on magnetic and dielectric properties of barium hexaferrite (BHF). *Physica B: Condensed Matter*, **579**; 411908

Kumar, S., M. Y. Wani, and J. Koh (2018). Synthesis of Nanomaterials Involving Microemulsion and Miceller Medium. In *Exploring the Realms of Nature for Nanosynthesis*. Springer International Publishing, pages 273–290

Li, H., L. Qin, Y. Feng, L. Hu, and C. Zhou (2015). Preparation and characterization of highly water-soluble magnetic Fe3O4 nanoparticles via surface double-layered self-assembly method of sodium alpha-olefin sulfonate. *Journal of Magnetism and Magnetic Materials*, **384**; 213–218

Li, L., K. Chen, H. Liu, G. Tong, H. Qian, and B. Hao (2013). Attractive microwave-absorbing properties of M-BaFe12O19 ferrite. *Journal of Alloys and Compounds*, **557**; 11–17

Li, Y., A. Xia, and C. Jin (2016). Synthesis, structure and magnetic properties of hexagonal BaFe12O19 ferrite obtained via a hydrothermal method. *Journal of Materials Science: Materials in Electronics*, **27**(10); 10864–10868

Lin, Y., X. Liu, T. Ye, H. Yang, F. Wang, and C. Liu (2016). Synthesis and characterization of graphene/0.8BaFe12O19/0.2Y3Fe5O12 nanocomposite. *Journal of Alloys and Compounds*, **683**; 559–566

Liu, Y., Y. Lin, and H. Yang (2019). Facile fabrication for core-shell BaFe12O19@C composites with excellent microwave absorption properties. *Journal of Alloys and Compounds*, **805**; 130–137

Liu, Z., Y. Pan, X. Li, J. Jie, and M. Zeng (2017). Chemical composition, antimicrobial and anti-quorum sensing activities of pummelo peel flavonoid extract. *Industrial Crops and Products*, **109**; 862–868

López-Téllez, G., P. Balderas-Hernández, C. E. Barrera-Díaz, A. R. Vilchis-Nestor, G. Roa-Morales, and B. Bilyeu (2013). Green Method to Form Iron Oxide Nanorods in Orange Peels for Chromium(VI) Reduction. *Journal of Nanoscience and Nanotechnology*, **13**(3); 2354–2361

Luthfianti, H. R., W. Widanarto, S. K. Ghoshal, M. Effendi, and W. T. Cahyanto (2020). Magnetic and microwave absorption properties of Mn4 doped barium-natural ferrites prepared by the modified solid-state reaction method. *Journal of Physics: Conference Series*, **1494**; 012043

Madhubala, V. and T. Kalaivani (2018). Phyto and hydrothermal synthesis of Fe3O4@ZnO core-shell nanoparticles using Azadirachta indica and its cytotoxicity studies. *Applied Surface Science*, **449**; 584–590

Madhumita, M., P. Guha, and A. Nag (2019). Extraction of betel leaves (Piper betle L.) essential oil and its bio-actives identification: Process optimization, GC-MS analysis and anti-microbial activity. *Industrial Crops and Products*, **138**; 111578

Madhumita, M., P. Guha, and A. Nag (2020). Bio-actives of betel leaf (Piper betle L.): A comprehensive review on extraction, isolation, characterization, and biological activity. *Phytotherapy Research*, **34**(10); 2609–2627

Manikandan, A., M. Durka, and S. A. Antony (2015). Hibiscus rosa-sinensis Leaf Extracted Green Methods, Magneto-Optical and Catalytic Properties of Spinel CuFe2O4 Nano- and Microstructures. *Journal of Inorganic and Organometallic Polymers and Materials*, **25**(5); 1019–1031

Marouani, Y., J. Massoudi, M. Noumi, A. Benali, E. Dhahri, P. Sanguino, M. P. F. Graça, M. A. Valente, and B. F. O. Costa (2021). Electrical conductivity and dielectric properties of Sr doped M-type barium hexaferrite BaFe12O19. *RSC Advances*, **11**(3); 1531–1542

Matzui, Trukhanov, Yakovenko, Vovchenko, Zagorodnii, Oliynyk, Borovoy, Trukhanova, Astapovich, Karpinsky, and Trukhanov (2019). Functional Magnetic Composites Based on Hexaferrites: Correlation of the Composition, Magnetic and High-Frequency Properties. *Nanomaterials*, **9**(12); 1720

Meng, X., Q. Han, Y. Sun, and Y. Liu (2019). Synthesis and microwave absorption properties of Ni0.5Zn0.5Fe2O4/BaFe12O19@polyaniline composite. *Ceramics International*, **45**(2); 2504–2508

Misra, T., S. Mitra, and S. Sen (2018). Adsorption studies of carbamazepine by green-synthesized magnetic nanosorbents. *Nanotechnology for Environmental Engineering*, **3**(1)

Mosleh, Z., P. Kameli, A. Poorbaferani, M. Ranjbar, and H. Salamati (2016). Structural, magnetic and microwave absorption properties of Ce-doped barium hexaferrite. *Journal of Magnetism and Magnetic Materials*, **397**; 101–107

Nikmanesh, H., S. Hoghoghifard, and B. Hadi-Sichani (2019). Study of the structural, magnetic, and microwave absorption properties of the simultaneous substitution of several cations in the barium hexaferrite structure. *Journal of Alloys and Compounds*, **775**; 1101–1108

Ovalioglu, H., H. Sozeri, M. Kabaer, and I. Kucuk (2010). Magnetic Properties of Nano-Crystalline Barium Ferrite Synthesized by Different Synthesis Route. *Acta Physica Polonica A*, **118**(5); 1020–1021

Ozah, S. and N. Bhattacharyya (2013). Nanosized barium hexaferrite in novolac phenolic resin as microwave absorber for X-band application. *Journal of Magnetism and Magnetic Materials*, **342**; 92–99

Pan, Z., Y. Wang, H. Huang, Z. Ling, Y. Dai, and S. Ke (2015). Recent development on preparation of ceramic inks in ink-jet printing. *Ceramics International*, **41**(10); 12515–12528

Peymanfar, R., A. Ahmadi, and E. Selseleh-Zakerin (2020). Evaluation of the size and medium effects on the microwave absorbing, magnetic, electromagnetic shielding, and optical properties using CuCo2S4 nanoparticles. *Journal of Alloys and Compounds*, **848**; 156453

Peymanfar, R., M. Ahmadi, and S. Javanshir (2019). Tailoring GO/BaFe12O19/La0.5Sr0.5MnO3 ternary nanocomposite and investigation of its microwave characteristics. *Materials Research Express*, **6**(8); 085063

Prasad, C., K. Sreenivasulu, S. Gangadhara, and P. Venkateswarlu (2017). Bio inspired green synthesis of Ni/Fe3O4 magnetic nanoparticles using Moringa oleifera leaves extract: A magnetically recoverable catalyst for organic dye degradation in aqueous solution. *Journal of Alloys and Compounds*, **700**; 252–258

Punuri, J. B., P. Sharma, S. Sibyala, R. Tamuli, and U. Bora (2012). Piper betle-mediated green synthesis of biocompatible gold nanoparticles. *International Nano Letters*, **2**(1)

Purba, . P. P., R. A. P. (2019). Bioanalytical HPLC method of Piper betle L. for quantifying phenolic compound, water-soluble vitamin, and essential oil in five different solvent extracts. *Journal of Applied Pharmaceutical Science*, **9**(5); 33–39

Rafiq, M. A., M. Waqar, T. A. Mirza, A. Farooq, and A. Zulfiqar (2016). Effect of Ni2+ Substitution on the Structural, Magnetic, and Dielectric Properties of Barium Hexagonal Ferrites (BaFe12O19). *Journal of Electronic Materials*, **46**(1); 241–246

Rahmayeni, R., Y. Oktavia, Y. Stiadi, S. Arief, and Z. Zulhadjri (2020). Spinel ferrite of MnFe2O4 synthesized in Piper betle Linn extract media and its application as photocatalysts and antibacterial. *Journal of Dispersion Science and Technology*, **42**(3); 465–474

Raj, B. D. P., K. Mallikarju, G. Dillip, G. Narasimha, and N. J. Sushma (2012). Phytofabrication and Characterization of Silver Nanoparticles from Piper betle Broth. *Research Journal of Nanoscience and Nanotechnology*, **2**(1); 17–23

Raja, D. and D. Sundaramurthy (2021). Facile synthesis of fluorescent carbon quantum dots from Betel leafs (Piper betle) for Fe^{3}+ sensing. *Materials Today: Proceedings*, **34**; 488–492

Ramasahayam, S. K., G. Gunawan, C. Finlay, and T. Viswanathan (2012). Renewable Resource-Based Magnetic Nanocomposites for Removal and Recovery of Phosphorous from Contaminated Waters. *Water, Air, & Soil Pollution*, **223**(8); 4853–4863

Rusianto, T., M. W. Wildan, K. Abraha, and K. Kusmono (2015). Characterizations of Ceramic Magnets from Iron Sand. *International Journal of Technology*, **6**(6); 1017

Sadishkumar, V. and K. Jeevaratnam (2016). In vitroprobiotic evaluation of potential antioxidant lactic acid bacteria isolated fromidlibatter fermented withPiper betleleaves. *International Journal of Food Science & Technology*, **52**(2); 329–340

Sarma, C., P. Rasane, S. Kaur, J. Singh, J. Singh, Y. Gat, U. Garba, D. Kaur, and K. Dhawan (2018). Antioxidant and antimicrobial potential of selected varieties of Piper betle L. (Betel leaf). *Anais da Academia Brasileira de Ciências*, **90**(4); 3871–3878

Saryanti, D., D. Nugraheni, and N. S. Astuti (2020). Preparation and Characterization of Betel Leaves (Piper betle Linn) Extract Nanoparticle with Ionic Gelation Method. *Journal of Tropical Pharmacy and Chemistry*, **5**(1)

Setiamukti, D., A. Khusnani, and M. Toifur (2020). The Effect of Electrolyte Concentration on The Sensitivity of Low-Temperature Sensor Performance of Cu/Ni Film. *Science and Technology Indonesia*, **5**(2); 28

Sharifi, I., H. Shokrollahi, and S. Amiri (2012). Ferrite-based magnetic nanofluids used in hyperthermia applications. *Journal* of Magnetism and Magnetic Materials, **324**(6); 903–915

Shejawal, K. P., D. S. Randive, S. D. Bhinge, M. A. Bhutkar, G. H. Wadkar, and N. R. Jadhav (2020). Green synthesis of silver and iron nanoparticles of isolated proanthocyanidin: its characterization, antioxidant, antimicrobial, and cytotoxic activities against COLO320DM and HT29. *Journal of Genetic Engineering and Biotechnology*, **18**(1)

Song, P., B. Liu, H. Qiu, X. Shi, D. Cao, and J. Gu (2021). MXenes for polymer matrix electromagnetic interference shielding composites: A review. *Composites Communications*, **24**; 100653

Susilawati, A. Doyan, and Khalilurrahman (2017). Synthesis and characterization of barium hexaferrite with manganese (Mn) doping material as anti-radar. Author(s)

Sözeri, H., Z. Mehmedi, H. Kavas, and A. Baykal (2015). Magnetic and microwave properties of BaFe 12 O 19 substituted with magnetic, non-magnetic and dielectric ions. *Ceramics International*, **41**(8); 9602–9609

Tagrida, M. and S. Benjakul (2020). Ethanolic extract of Betel (Piper betle L.) and Chaphlu (Piper sarmentosum Roxb.) dechlorophyllized using sedimentation process: Production, characteristics, and antioxidant activities. *Journal of Food Biochemistry*, **44**(12)

Thakur, A., N. Sharma, M. Bhatti, M. Sharma, A. V. Trukhanov, S. V. Trukhanov, L. V. Panina, K. A. Astapovich, and P. Thakur (2020). Synthesis of barium ferrite nanoparticles using rhizome extract of Acorus Calamus: Characterization and its efficacy against different plant phytopathogenic fungi. *Nano-Structures & Nano-Objects*, **24**; 100599

Ting, T.-H. and K.-H. Wu (2010). Synthesis, characterization of polyaniline/BaFe12O19 composites with microwave-absorbing properties. *Journal of Magnetism and Magnetic Materials*, **322**(15); 2160–2166

Torabi, Z., A. Arab, and F. Ghanbari (2017). Structural, Magnetic and Microwave Absorption Properties of Hydrothermally Synthesized (Gd, Mn, Co) Substituted Ba-Hexaferrite Nanoparticles. *Journal of Electronic Materials*, **47**(2); 1259–1270

Ullah, A., S. Munir, S. L. Badshah, N. Khan, L. Ghani, B. G. Poulson, A.-H. Emwas, and M. Jaremko (2020). Important Flavonoids and Their Role as a Therapeutic Agent. *Molecules*, **25**(22); 5243

Vinnik, D., D. Klygach, V. Zhivulin, A. Malkin, M. Vakhitov, S. Gudkova, D. Galimov, D. Zherebtsov, E. Trofimov, N. Knyazev, V. Atuchin, S. Trukhanov, and A. Trukhanov (2018). Electromagnetic properties of BaFe12O19:Ti at centimeter wavelengths. *Journal of Alloys and Compounds*, **755**; 177–183

Vinnik, D., A. Trukhanov, F. Podgornov, E. Trofimov, V. Zhivulin, A. Starikov, O. Zaitseva, S. Gudkova, A. Kirsanova, S. Taskaev, D. Uchaev, S. Trukhanov, M. Almessiere, Y. Slimani, and A. Baykal (2020). Correlation between entropy state, crystal structure, magnetic and electrical properties in M-type Ba-hexaferrites. *Journal of the European Ceramic Society*, **40**(12); 4022–4028

Wang, L., X. Huang, J. Zhang, H. Wang, Q. Zhang, and N. Xu (2011). Microstructure and microwave electromagnetic properties of Dy3 -doped W-type hexaferrites. *Rare Metals*, **30**(5); 505–509

Wang, M., Y. Lin, H. Yang, Y. Qiu, and S. Wang (2020). A novel plate-like BaFe12O19@MoS2 core-shell structure composite with excellent microwave absorbing properties. *Journal of Alloys and Compounds*, **817**; 153265

Wu, N., Q. Hu, R. Wei, X. Mai, N. Naik, D. Pan, Z. Guo, and Z. Shi (2021). Review on the electromagnetic interference shielding properties of carbon based materials and their novel composites: Recent progress, challenges and prospects. *Carbon*, **176**; 88–105

Xu, Y., F. Ge, M. Xie, S. Huang, J. Qian, H. Wang, M. He, H. Xu, and H. Li (2019). Fabrication of magnetic BaFe12O19/Ag3PO4 composites with an in situ photo-Fenton-like reaction for enhancing reactive oxygen species under visible light irradiation. *Catalysis Science & Technology*, **9**(10); 2563–2570

Yang, C., Y. Gung, C. Shih, W. Hung, and K. Wu (2011). Synthesis, infrared and microwave absorbing properties of (BaFe12O19+BaTiO3)/polyaniline composite. *Journal of Magnetism and Magnetic Materials*, **323**(7); 933–938

Yang, H., T. Ye, Y. Lin, and M. Liu (2015). Preparation and microwave absorption property of graphene/BaFe12O19/CoFe2O4 nanocomposite. *Applied Surface Science*, **357**; 1289–1293

Yang, X., M. Ge, J. Zhang, B. Jia, and F. Bu (2019). Fabrication of Al2O3@BaFe12O19 core-shell powder by a modified heterogeneous precipitation method. *Ceramics International*, **45**(3); 3269–3275

Yang, Y. and J. Wang (2014). Synthesis and characterization of a microwave absorbing material based on magnetoplumbite ferrite and graphite nanosheet. *Materials Letters*, **124**; 151–154

Yin, L., T. Chen, S. Liu, Y. Gao, B. Wu, Y. Wei, G. Li, X. Jian, and X. Zhang (2015). Preparation and microwave-absorbing property of BaFe12O19 nanoparticles and BaFe12O19/Fe3C/CNTs composites. *RSC Advances*, **5**(111); 91665–91669

Zhao, L., X. Lv, Y. Wei, C. Ma, and L. Zhao (2013). Hydrothermal synthesis of pure BaFe12O19 hexaferrite nanoplatelets under high alkaline system. *Journal of Magnetism and Magnetic Materials*, **332**; 44–47

Zhao, T., X. Ji, W. Jin, C. Wang, W. Ma, J. Gao, A. Dang, T. Li, S. Shang, and Z. Zhou (2017). Direct in situ synthesis of a 3D interlinked amorphous carbon nanotube/graphene/BaFe12O19 composite and its electromagnetic wave absorbing properties. *RSC Advances*, **7**(26); 15903–15910

Zhu, X., X. Wang, K. Liu, M. Meng, and M. N. Akhtar (2020). Microwave absorption characteristics of carbon foam decorated with BaFe12O19 and Ni0.5Co0.5Fe2O4 magnetic composite in X-band frequency. *Journal of Magnetism and Magnetic Materials*, **513**; 167258

